Journal of Power Sources 266 (2014) 222–225

Contents lists available at ScienceDirect

Journal of Power Sources

journal homepage: www.elsevier.com/locate/jpowsour

Short communication

A high activity nitrogen-doped carbon catalyst for oxygen reduction reaction derived from polyaniline-iron coordination polymer

Guanghua Wang, Kezhu Jiang, Mingli Xu, Chungang Min, Baohua Ma, Xikun Yang*

Research Center for Analysis and Measurement, Kunming University of Science and Technology, Kunming 650093, PR China

HIGHLIGHTS

- A nitrogen-doped carbon catalyst derived from PANI-iron coordination polymer.
- Fe was uniformly distributed in precursor by coordination between Fe^{3+} and PANI.
- N/C/Fe-*c* catalyst exhibits comparable diffusion-limited current density to Pt/C.

GRAPHICAL ABSTRACT

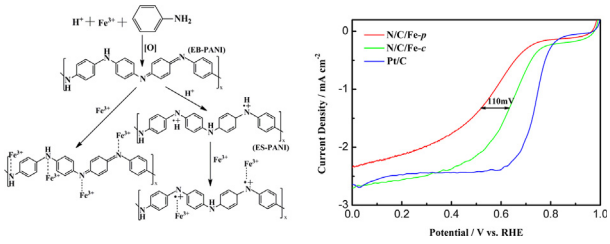

ARTICLE INFO

Article history:
Received 22 January 2014
Received in revised form
25 April 2014
Accepted 6 May 2014
Available online 15 May 2014

Keywords:
Nitrogen-doped carbon catalyst
Coordination polymer
Homogenous active sites
Oxygen reduction reaction

ABSTRACT

A nitrogen-doped carbon catalyst with trace iron (N/C/Fe-*c*, 0.54 wt.% Fe) has been prepared through pyrolysis of polyaniline (PANI)-iron coordination polymer. Electrochemical results demonstrate that N/C/Fe-*c* catalyst displays excellent oxygen reduction reaction (ORR) catalytic activity and shows almost the same diffusion-limited current density for ORR as Pt/C catalyst in acid media. FTIR and XPS measurements indicate that Fe^{3+} ions coordinate with N atoms of the PANI chains and N/C/Fe-*c* has a high ratio of graphitic N, which are responsible for high ORR activity.

1. Introduction

Nitrogen-doped carbon catalysts possess great potential for ORR catalyst in fuel cells application due to their high efficiency, durable performance and low cost [1,2]. These catalysts are obtained via pyrolysis of the precursor containing nitrogen source, carbon source and transition metals [3,4]. Introduction of transition metals (Fe and/or Co) into the precursor can markedly promote ORR catalytic activity of nitrogen-doped carbon catalysts. Although actual role of the transition metals in nitrogen-doped carbon catalysts is still a controversial issue, there is a consensus that transition metals are needed to create active sites during the heat treatment [5]. Transition metals content does not always correlate to the ORR activity. For instance, Fe content beyond 3 wt.% limits the formation of active sites and the specific surface area of catalyst decreases with the increase of Fe content [6,7]. Transition metals are mainly added into the precursor by physical mixing method and impregnation method. For physical method [8,9], transition metals can not be distributed homogenously into the precursor and excessive residual metals need be removed by acid washing. For impregnation method [10,11], transition metals merely exist on the surface of precursor and the amount of adsorbed transition metals is too low. These methods will lead to inhomogenous distribution of transition metals, and thus can not adequately produce plenty of homogenous

* Corresponding author. Tel.: +86 0871 65110975; fax: +86 0871 65111617.
E-mail address: yxk630@hotmail.com (X. Yang).

http://dx.doi.org/10.1016/j.jpowsour.2014.05.020
0378-7753/

ORR active sites along with heat treatment. Therefore, it is very important to explore new precursor preparation approaches to obtain high activity nitrogen-doped carbon catalyst.

In general, PANI containing transition metals and carbon supports (such as carbon black, carbon nanotube or graphene) has been used as precursor to prepare electrocatalyst for ORR [12]. Most of the precursors derived from PANI are prepared by physical method and a large number of transition metals are retained in the precursors. This would result in the formation of relatively unstable phases during heat treatment [6]. It is well known that PANI chains have two kinds of nitrogen atoms: the imine nitrogen atoms (N═Q═N) of the quinoid rings and the amine nitrogen atoms (HN–B–NH) of the benzenoid rings (Q = quinoid rings, B = benzenoid rings) [13]. PANI can coordinate with transition metal ions [14]. For example, when Fe^{3+} ions are added into the synthesized system of PANI polymer, Fe^{3+} ions can coordinate with both the imine N and the amine N atoms of the PANI chains [15], which forms PANI-iron coordination polymer. Thus, Fe can be uniformly distributed in PANI by this chemical method. Based this idea, herein a new precursor of PANI coordinating with Fe^{3+} ions was used to prepare high activity nitrogen-doped carbon catalyst (0.54 wt.% Fe) for ORR. The obtained catalyst showed a high activity toward the ORR due to homogenous distribution of Fe in the precursor by coordination between Fe^{3+} and PANI.

2. Experimental

2.1. Synthesis of catalysts

The PANI-iron coordination polymer was synthesized according to the literature where $(NH_4)_2S_2O_8$ was used as oxidant [16]. 10 mL of aniline was first dissolved in 200 mL of 1 M H_2SO_4 solution containing 5 mmol $NH_4Fe(SO_4)_2{\cdot}12H_2O$. The molar ratio of Fe to aniline was 1:20. Then, 4.63 g of $(NH_4)_2S_2O_8$ (dissolved in 50 mL of 1 M H_2SO_4 solution) was added into the above solution with constant stirring. The suspension was kept at 0–5 °C for 24 h. The precipitate was filtered and washed with deionized water for three times, then dried at 60 °C for 24 h under vacuum. PANI was prepared following the above process in 1 M H_2SO_4 solution without $NH_4Fe(SO_4)_2{\cdot}12H_2O$. The mixture of iron and PANI was prepared by physical method: 0.5 g PANI powders and 0.17 g $NH_4Fe(SO_4)_2{\cdot}12H_2O$ were ballmilled for 3 h in a solution of ethanol and deionized water (1:2 ethanol/H_2O), then the mixture was dried at 60 °C for 24 h under vacuum. Finally, PANI-iron coordination polymer and the mixture were pyrolyzed at 900 °C in nitrogen gas for 1 h and corresponding samples were denoted as N/C/Fe-*c* and N/C/Fe-*p*, respectively. The contents of Fe in N/C/Fe-*c* and N/C/Fe-*p* measured by ICP-AES were 0.54 wt.% and 6.12 wt.%, respectively.

2.2. Physical and electrochemical characterizations

Fourier transform infrared (FT-IR, AVATAR 360 FT-IR), Transmission electron microscope (TEM, JEM-2100/UHR), X-ray photoelectron spectroscope (XPS, PHI-5000 VersaProbe II) and Inductively coupled plasma emission spectrometer (ICP-AES, PS1000) were used to characterize the coordination structure of the PANI and PANI-iron coordination polymer, the morphology, surface chemical state and the iron concentrations of the catalysts.

Cyclic voltammogram (CV) and linear sweep voltammogram (LSV) were measured in a conventional three-electrode system with 0.5 M H_2SO_4 electrolyte at room temperature. A platinum wire and an Ag/AgCl electrode were used as the counter electrode and reference electrode, respectively. The catalyst-coated glassy carbon (GC 4.0 mm diameter) electrode was used as the working electrode. The catalyst ink was prepared by ultrasonically mixing 6 mg of catalyst powders with 950 mL of isopropyl alcohol and 50 mL of 5 wt.% Nafion solution for 30 min. 10 μL of the ink was deposited onto the GC surface and dried in air at room temperature. For comparison, a commercially available Pt/C catalyst (20 wt.% Pt, Johnson-Matthey) was used under the same conditions.

3. Results and discussion

3.1. FTIR analyst

The FTIR spectra of the PANI and PANI-iron coordination polymer were shown in Fig. 1(A). PANI had two typical absorption peaks appeared at 1303 cm^{-1} and 1160 cm^{-1}, which were assigned to the N–H bending mode and the –N═ vibration, respectively [17]. Compared with PANI, the spectrum of PANI-iron coordination polymer had an obvious difference. The peaks at 1303 cm^{-1} and 1160 cm^{-1} in PANI shifted to 1300 cm^{-1} and 1145 cm^{-1} in PANI-iron coordination polymer. The red shift of two absorption peaks of PANI-iron coordination polymer was due to coordinative interaction of N atoms with Fe^{3+} ions [14]. This could be explained as follows: Fe^{3+} could directly coordinate with imine N atoms and amine N atoms of the emeraldine base (EB-PANI) chains through both pseudo-protonation and amine oxidation process [15]. On the other hand, EB-PANI could be doped by protonic acids, leading to emeraldine salt (ES-PANI). According to Pearson's hard soft acid base principle [18], hard acids prefer to bind to hard bases and soft acids prefer to bind to soft bases. It is known that Fe^{3+} is hard acid [18] and ES-PANI is hard base [19]. Therefore, Fe^{3+} could coordinate with the N atoms of ES-PANI chains. The similar coordination between transition metal ions and PANI had been reported [16,20]. The proposed reaction of the PANI-iron coordination polymer could be depicted as shown in Fig. 1(B). As a result of the formation of PANI-iron coordination polymer, Fe would be uniformly distributed in the PANI at the molecular level.

3.2. TEM and XPS analysts

Low-resolution TEM images of N/C/Fe-*c* and N/C/Fe-*p* were shown in Fig. 2. Besides the presence of amorphous carbon particles, some dark spots could be observed in the N/C/Fe-*c* (Fig. 2(A)). While we could not find the crystallite structure of Fe species by high-resolution TEM (HR-TEM, inset of Fig. 2(A)). The dark spot might be the piling of carbon spherical particles [9]. However, it could be seen that clear metallic particles with crystallite structure were covered by carbon layer in the N/C/Fe-*p* (Fig. 2(B)). The inset HR-TEM image of Fig. 2(B) showed that the interplanar spacing of the nanoparticle was 0.286 nm, which corresponded to the (220) plane of Fe_3O_4.

XPS spectra of N1s region for N/C/Fe-*c* and N/C/Fe-*p* were shown in Fig. 2(C) and (D). The N/C atomic ratios at the surface of N/C/Fe-*c* and N/C/Fe-*p* were 3.30 at.% and 2.62 at.%, respectively. It indicated that the total content of N in N/C/Fe-*c* was higher than that of N/C/Fe-*p*. The N1s peak of N/C/Fe-*c* could be deconvoluted into three peaks: graphitic N (401.28 eV, 79.85 at.%), pyrrolic N (399.86 eV, 9.17 at.%) and pyridinic N (398.10 eV, 10.98 at.%) [21–23]. For N/C/Fe-*p*, the three peaks were graphitic N (401.22 eV, 50.63 at.%), pyrrolic N (400.37 eV, 18.93 at.%) and pyridinic N (398.36 eV, 30.44 at.%). Compared with N/C/Fe-*p*, N/C/Fe-*c* had a higher ratio of graphitic-N which made a major contribution to the ORR activity [24,25].

3.3. Electrochemical activity for ORR

The continuous CV curves of N/C/Fe-*c* and N/C/Fe-*p* catalysts in nitrogen saturated 0.5 M H_2SO_4 were presented in Fig. 3(A). CV

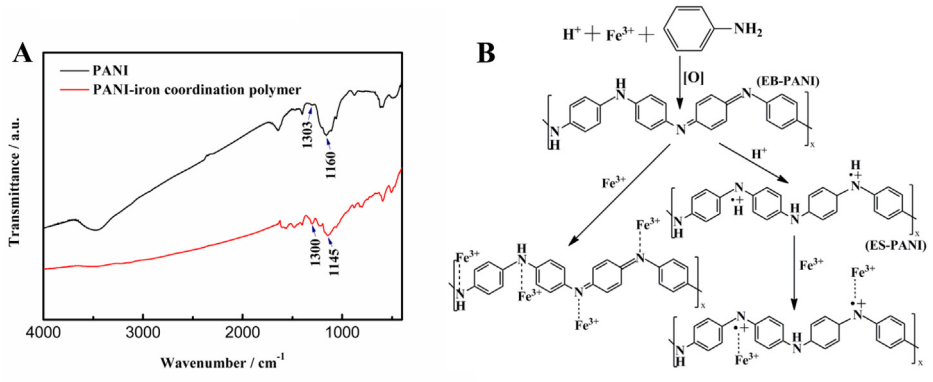

Fig. 1. (A) FTIR spectra of the PANI and PANI-iron coordination polymer. (B) Schematic illustration of the proposed reaction of the PANI-iron coordination polymer: Fe^{3+} ions coordinate with the N atoms of the PANI chains.

curves of both catalysts showed a pair of well-defined redox peaks at about ca. 0.60 V, which could be attributed to the Fe^{3+}/Fe^{2+} redox couple [2]. After 50 cycles, the redox peak potential of N/C/Fe-*c* had no obvious changes, and the CV curve area of N—C—Fe-*c* increased. However, the corresponding redox peak potential of N/C/Fe-*p* had an obvious shift and CV curve area of N/C/Fe-*p* decreased. This implied that iron oxides in the N/C/Fe-*p* catalyst were partially dissolved in 0.5 M H_2SO_4.

The LSV curves of N/C/Fe-*c* and N/C/Fe-*p* catalysts in oxygen saturated 0.5 M H_2SO_4 were presented in Fig. 3(B). The onset potential, half-wave potential and diffusion-limited current density of N—C—Fe-*c* catalyst were 0.78 V, 0.65 V and 2.7 mA cm^{-2}, respectively. Furthermore, 110 mV positive shift of half-wave potential and 0.4 mA cm^{-2} increase of limiting current density had been achieved compared to those of N/C/Fe-*p* catalyst. N/C/Fe-*c* catalyst displayed lower onset potential and half-wave potential than those of commercial 20 wt.% Pt/C catalyst. However, the N/C/Fe-*c* catalyst achieved almost the same diffusion-limited current density as that of Pt/C catalyst. Although Fe content of N/C/Fe-*p* was roughly 10 times higher than that of N/C/Fe-*c*, the N/C/Fe-*p* catalyst showed much lower catalytic activity than N/C/Fe-*c* catalyst in 0.5 M H_2SO_4. This could be attributed to the fact that excess of Fe supply would form the non-active phase and limit the formation of active sites [6,11]. For the N/C/Fe-*c* catalyst, homogenous distribution of Fe in the PANI-iron coordination polymer could generate a large amount of homogenized ORR active sites during the heat treatment, and thus the obtained catalyst exhibited a high catalytic activity.

The kinetic analysis of ORR at N/C/Fe-*c* and N/C/Fe-*p* catalysts were investigated using the rotating disk electrode from 900 to 3000 rpm. Fig. 3(C) showed the LSV curves of N/C/Fe-*c* catalyst. The Koutecky—Levich plots (j^{-1} vs. $\omega^{-1/2}$) of N/C/Fe-*c* catalyst at different electrode potentials were presented in the inset of Fig. 3(C). According to Koutecky—Levich equations [26], the average *n* values of N/C/Fe-*c* and N/C/Fe-*p* catalysts were calculated to be 3.6

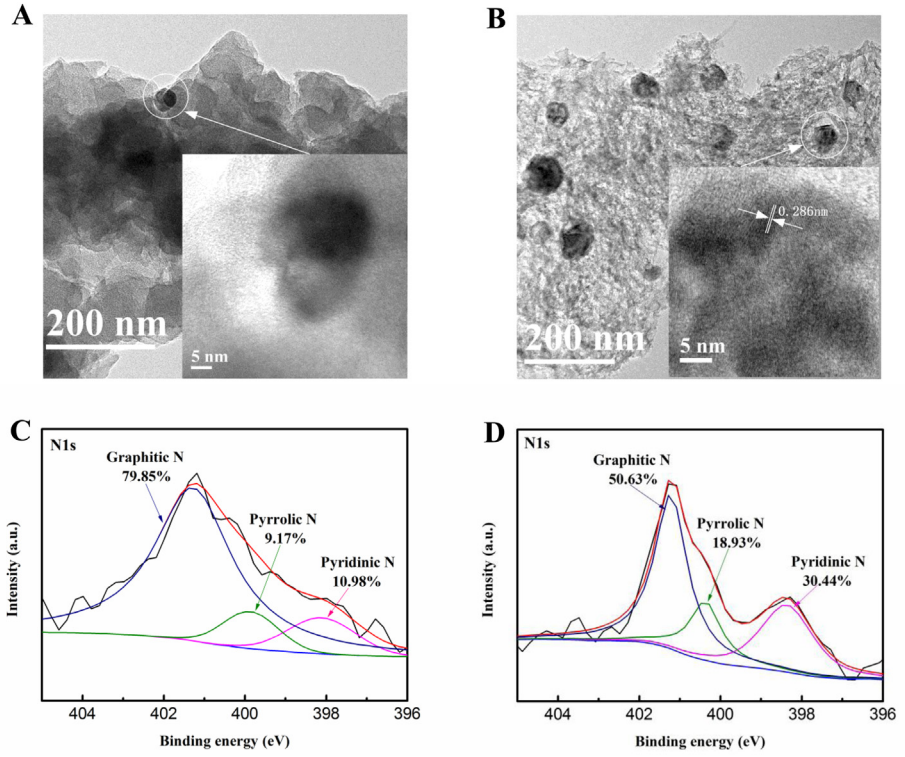

Fig. 2. TEM images of N/C/Fe-*c* (A) and N/C/Fe-*p* (B) (inset is HR-TEM image of Fe_3O_4 nanoparticle). XPS spectra of N1s region for N/C/Fe-*c* (C) and N/C/Fe-*p* (D).

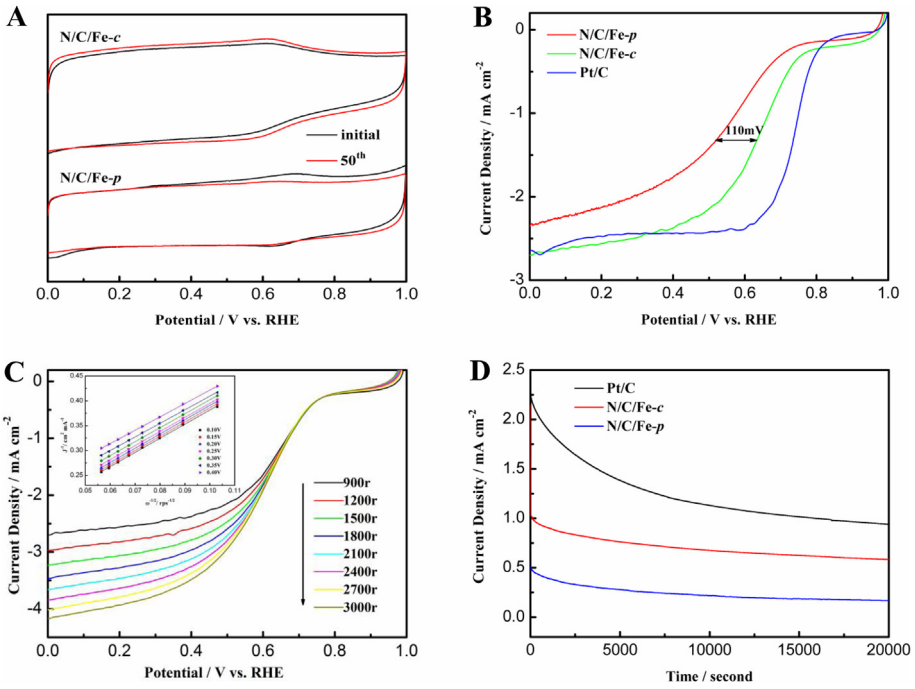

Fig. 3. (A) CVs recorded for N/C/Fe-*c* and N/C/Fe-*p* catalysts in N_2-saturated 0.5 M H_2SO_4 solution. (B) Comparative LSVs at 900 rpm for N/C/Fe-*c* and N/C/Fe-*p* catalysts along with commercial 20 wt.% Pt/C catalyst. (C) LSVs of N/C/Fe-*c* catalyst in O_2-saturated 0.5 M H_2SO_4 solution at various rotation speeds. Inset is the corresponding Koutecky–Levich plots. (D) Chronoamperometric curves of N/C/Fe-*c*, N/C/Fe-*p* and Pt/C catalysts in O_2-saturated 0.5 M H_2SO_4 solution at 5 mV s^{-1} and 900 rpm.

and 3, respectively. The number of electrons transfer for N/C/Fe-*c* catalyst was closed to 4, which revealed that the ORR on N/C/Fe-*c* catalyst mainly followed the 4 electrons transfer process.

The chronoamperometric curves of N/C/Fe-*c*, N/C/Fe-*p* and Pt/C catalysts at 0.6 V were recorded to study the ORR durability (Fig. 3(D)). The N/C/Fe-*c* and N/C/Fe-*p* catalysts showed only a negligible current decay, while the commercial Pt/C catalyst revealed a significant current decay. It was clear that the current density of N/C/Fe-*c* catalyst was higher than that of N/C/Fe-*p* catalyst in the whole process. This indicated that the N/C/Fe-*c* catalyst had better performance compared to N/C/Fe-*p* catalysts.

4. Conclusions

A nitrogen-doped carbon catalyst with trace iron was derived from PANI-iron coordination polymer. The resulting catalyst exhibited excellent electrocatalytic performance for ORR in acid media, which can be attributed to the presence of a large amount of homogenous active site created by the homogenous distribution of Fe in PANI-iron coordination polymer. The catalyst mainly followed 4 electrons transfer process. This work offers a novel route to design and development of nitrogen-doped carbon catalysts for ORR.

Acknowledgments

This work was financially supported by the National Scientific Foundation of China (NSFC Project Nos. 21363012, 51374117, 51164017).

References

[1] E. Proietti, F. Jaouen, M. Lefèvre, N. Larouche, J. Tian, J. Herranz, J.P. Dodelet, Nat. Commun. 2 (2011) 416.
[2] G. Wu, K.L. More, C.M. Johnston, P. Zelenay, Science 332 (2011) 443–447.
[3] K. Niu, B. Yang, J. Cui, J. Jin, X. Fu, Q. Zhao, J. Zhang, J. Power Sources 243 (2013) 65–71.
[4] S. Li, Y. Hu, Q. Xu, J. Sun, B. Hou, Y. Zhang, J. Power Sources 213 (2012) 265–269.
[5] F. Jaouen, E. Proietti, M. Lefèvre, R. Chenitz, J.P. Dodelet, G. Wu, H.T. Chung, C.M. Johnston, P. Zelenay, Energy Environ. Sci. 4 (2011) 114–130.
[6] G. Wu, C.M. Johnston, N.H. Mack, K. Artyushkova, M. Ferrandon, M. Nelson, J.S. Lezama-Pacheco, S.D. Conradson, K.L. More, D.J. Myers, P. Zelenay, J. Mater. Chem. 21 (2011) 11392–11405.
[7] G.Q. Sun, J.T. Wang, S. Gupta, R.F. Savinell, J. Appl. Electrochem. 31 (2001) 1025–1031.
[8] M. Lefèvre, E. Proietti, F. Jaouen, J.P. Dodelet, Science 324 (2009) 71–74.
[9] H. Xiao, Z.G. Shao, G. Zhang, Y. Gao, W. Lu, B. Yi, Carbon 57 (2013) 443–451.
[10] J.S. Lee, G.S. Park, S.T. Kim, M. Liu, J. Cho, Angew. Chem. Int. Ed. 52 (2013) 1026–1030.
[11] Y. Hu, X. Zhao, Y. Huang, Q. Li, N.J. Bjerrum, C. Liu, W. Xing, J. Power Sources 225 (2013) 129–136.
[12] G. Wu, K. Artyushkova, M. Ferrandon, J. Kropf, D. Myers, P. Zelenay, ECS Trans. 25 (1) (2009) 1299–1311.
[13] J.-C. Chiang, A.G. Macdiarmid, Synth. Met. 13 (1986) 193–205.
[14] D. Ghosh, S. Giri, A. Mandal, C.K. Das, Appl. Surf. Sci. 276 (2013) 120–128.
[15] C.M.S. Izumi, V.R.L. Constantino, A.M.C. Ferreira, M.L.A. Temperini, Synth. Met. 156 (2006) 654–663.
[16] L. Tang, T. Wu, J. Kan, Synth. Met. 159 (2009) 1644–1648.
[17] S. Tao, B. Hong, Z. Kerong, Spectrochim. Acta Part A 66 (2007) 1364–1368.
[18] R.G. Pearson, J. Chem. Educ. 45 (1968) 581–587.
[19] M.M. Chehimi, M.-L. Abel, C. Perruchot, M. Delamar, S.F. Lascelles, S.P. Armes, Synth. Met. 104 (1999) 51–59.
[20] S. Giri, D. Ghosh, C.K. Das, J. Electroanal. Chem. 697 (2013) 32–45.
[21] J. Casanovas, J.M. Ricart, J. Rubio, F. Illas, J.M. Jiménez-Mateos, J. Am. Chem. Soc. 118 (1996) 8071–8076.
[22] V. Nallathambi, J.-W. Lee, S.P. Kumaraguru, G. Wu, B.N. Popov, J. Power Sources 183 (2008) 34–42.
[23] J. Wang, S. Li, G. Zhu, W. Zhao, R. Chen, M. Pan, J. Power Sources 240 (2013) 381–389.
[24] T. Iwazaki, R. Obinata, W. Sugimoto, Y. Takasu, Electrochem. Commun. 11 (2009) 376–378.
[25] R. Liu, D. Wu, X. Feng, K. Müllen, Angew. Chem. Int. Ed. 49 (2010) 2565–2569.
[26] Z.F. Ma, X.Y. Xie, X.X. Ma, D.Y. Zhang, Q. Ren, N. Heß-Mohr, V.M. Schmidt, Electrochem. Commun. 8 (2006) 389–394.